Springer

KSME

Journal of Mechanical Science and Technology 26 (6) (2012) 1793~1800
www.springerlink.com/content/1738-494x
DOI 10.1007/s12206-012-0420-9

High-efficiency design of a tunnel ventilation jet fan through numerical optimization techniques †

Joon-Hyung Kim[1,2], Jin-Hyuk Kim[3], Kwang-Yong Kim[3], Joon-Yong Yoon[1], Sang-Ho Yang[4] and Young-Seok Choi[2,*]

[1]*Department of Mechanical Engineering, Hanyang University, Seoul, Korea*
[2]*Green Energy System Technology Center, KITECH, Cheonan, Korea*
[3]*Department of Mechanical Engineering, Inha University, Incheon, Korea*
[4]*Technology Research Center, Samwon E&B, Shihung, Korea*

(Manuscript Received August 25, 2011; Revised December 20, 2011; Accepted February 21, 2012)

Abstract

This paper describes a numerical optimization procedure for performance improvement of a tunnel ventilation jet fan. We employ optimization techniques based on a PRESS (predicted error sum of squares)-based-averaging (PBA) model to improve the aerodynamic performance of a tunnel ventilation jet fan. For numerical analyses, three-dimensional Reynolds-averaged Navier-Stokes (RANS) equations with a shear stress transport turbulence model are discretized using finite volume approximations and solved on hexahedral grids to evaluate the total efficiency at operating conditions as the objective function. Numerical results are verified by using experimental data for the total efficiency and the effective outlet velocity at operating conditions. Further, four geometric variables are used defining the meridional length and the thickness profile at the hub and shroud in the jet fan rotor as the design variables for numerical optimization. The results of numerical optimization show a significant improvement in the total efficiency of the optimum model in comparison with the base model.

Keywords: Jet fan; Tunnel ventilation; Numerical optimization; Performance improvement; Total efficiency; Effective outlet velocity

1. Introduction

Ventilation is an important factor in contemporary tunnel construction as tunnels become longer and tunnel traffic increases. Tunnel ventilation serves several purposes. First, ventilation discharges pollutants from tunnels to maintain a comfortable, safe driving environment. Secondly, ventilation reduces concentrations of pollutants to acceptable levels to further ensure the safety of humans during maintenance work. Finally, ventilation discharges smoke from tunnels during emergencies.

These reasons reveal the mandatory nature of appropriate ventilation plans when designing and constructing tunnels. We divide tunnel ventilation methods into natural ventilation and mechanical ventilation. In general, the piston effect of cars running inside tunnels of shorter than 500 m can naturally ventilates the structure. However, newer tunnels tend to run longer than 500 m, causing a need for mechanical ventilation to maintain a comfortable and safe environment [1].

Mechanical ventilation methods include longitudinal, semi-transverse and transverse methods. Europe, Japan, and Korea employ longitudinal ventilation methods using low-cost, highly efficient jet fans. In longitudinal ventilation, jet fans installed in tunnels at certain intervals propel fast-flowing air that produces kinetic energy and thus facilitates ventilation. Longitudinal ventilation methods not only make it possible to reduce tunnel sectional area compared to semi-transverse and transverse methods but also result in reduced construction and operational costs since they do not need individual air inlets and outlets [2].

The jet fans mentioned serve as air blowers installed in the ceiling or walls of tunnels and underground roadways to provide ventilation. They work in a way similar to axial fans; however, the difference lies in the rotating speed of the jet fans since great quantities air must be discharged. Recent technology has set about reducing the maintenance cost of these jet fans as they must provide ventilation for many hours in place in the tunnels. Accordingly, researchers labor to improve the efficiency of the jet fan in Europe and Japan [3-5]. The trend is that the developer or research institutes even in the country are doing research into jet fans [6, 7].

*Corresponding author. Tel.: +82 41 589 8337, Fax.: +82 41 589 8330
E-mail address: yschoi@kitech.re.kr
† Recommended by Associate Editor Byeong Rog Shin

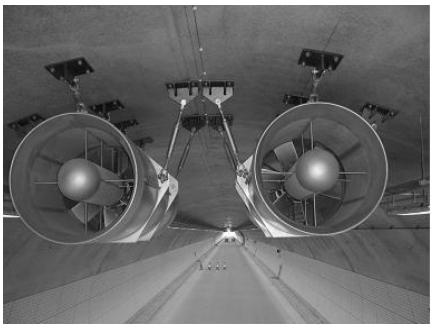

(a) Installed jet fan

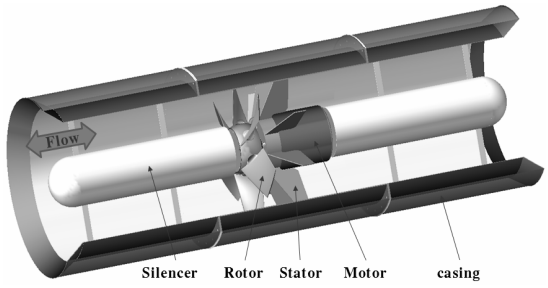

(b) Jet fan geometry

Fig. 1. Description of a general jet fan.

This work suggests guidelines for the high-efficiency design of a tunnel ventilation jet fan through numerical optimization techniques. Prior to numerical optimization, we validate the result of numerical analysis by comparing it to experimental data of operating conditions of the jet fan. Four geometric variables related to the meridional length and the thickness profile at the hub and shroud in the jet fan rotor serve as design variables. Finally, we explore and discuss optimization techniques based on a PRESS (predicted error sum of squares)-based-averaging (PBA) model combined with three-dimensional Reynolds-averaged Navier-Stokes (RANS) analysis to improve the total efficiency of a tunnel ventilation jet fan.

2. Design concepts of a tunnel ventilation jet fan

2.1 Operating system

As shown in Fig. 1, jet fans consist of a casing that holds a silencer, a rotor, a motor as power source, and a stator that fixes the motor to the casing. The total assembly hangs from the ceiling of a tunnel. Hence, jet fans must be safe and durable, especially because they hang in place in operation over a long period.

Jet fans, similar to axial fans in shape, rotate faster to create a very high speed of airflow. Limited in size, they have silencers on two sides to reduce flow noise. Also, jet fans must have reversibility to discharge smoke in case of fire. All of these features make jet fans technology-intensive products.

Table 1. Design specifications of the base model.

Number of rotor blades (EA)	6
Number of stator blades (EA)	9
Rotor tip clearance (mm)	5
Blade angle of hub (degree)	46.8
Blade angle of shroud (degree)	22.1
Meridional length of hub (mm)	94
Meridional length of shroud (mm)	48.6
Maximum thickness of hub (mm)	28
Maximum thickness of shroud (mm)	10

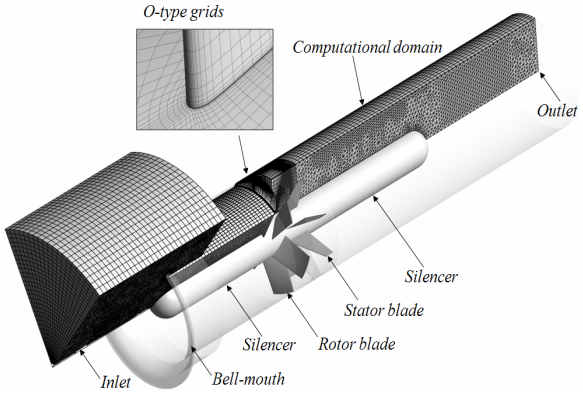

Fig. 2. Computational domain and grid system of the jet fan.

2.2 Design specifications of the base model

This study uses the base model from a previous work as its reference [8] prior to performing design optimization of the jet fan. The jet fan rotor of the base model operates at 1780 rpm rotating speed. The effective outlet velocity and the total efficiency at operating conditions are 36 m/s and 68%, respectively. Table 1 lists the detailed specifications of the base model.

3. Numerical analysis method

The flow analysis is carried out using ANSYS CFX Ver. 12, a three-dimensional viscous fluid analysis program. To examine the characteristics of the internal flow fields of the rotor and stator, three-dimensional RANS equations are used to analyze the incompressible turbulent flow. The governing equations with the shear stress transport k-ω model used in the numerical analysis are discretized by a finite volume method using a high-resolution scheme with second-order. The shear stress transport k-ω model, having the advantages of both k-ω and k-ε, employs the k-ω model at the near-wall and the k-ε model in the bulk-flow regions, a blending function ensuring a smooth transition between the two models [9].

Fig. 2 shows the computational domain for the numerical analysis. The rotor to be modeled has six blades and the stator nine blades. Numerical analysis of the flow passage of one

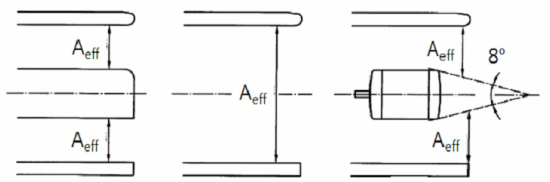

Fig. 3. Definition of the effective outlet area.

rotor and two stators was conducted using periodic conditions, taking analysis time into consideration [10]. Frozen rotor interfaces between the inlet-rotor and rotor-stator domains are applied to simulate different relative flow domains. General grid interface (GGI) is applied to interface conditions about each flow region. Standard air is considered as the working fluid and the total and static atmosphere pressures are set at the inlet and outlet flow region, respectively, for boundary conditions. For the numerical analysis of the jet fan, the atmosphere pressure conditions at the inlet and outlet should be applied, since the jet fan is not connected with other systems. The rotation speed of the rotor is 1780 rpm.

As shown in Fig. 2, a grid structure system of the rotor and stator is constructed using ANSYS Turbo-Grid ver. 12, which has O-type grids near the blade surface and hexahedral grids in the region of the rotor and stator. Construction of the flow regions of the inlet and outlet uses ANSYS CFX-Mesh ver. 11 on tetrahedral grids. The optimum grid system selected by the grid dependency test has 320,000 grids, as reported in a previous work [11].

Root mean squared residual values of the momentum and mass are set to fall below 1.0E-06. The converged solutions are obtained after approximately 500 iterations. The computations using a PC with an Intel Xeon (R) CPU clock speed of 2.67 GHz. The computational time is about 3 hours depending on the geometry considered and the rate of convergence.

4. Optimization techniques

4.1 Objective function

In this study, the aerodynamic performance parameters of a tunnel ventilation jet fan are typically represented as the effective outlet velocity (V_{eff}) and the total efficiency (η_t) as follows:

$$V_{eff} = \frac{Q}{A_{eff}}, \tag{1}$$

$$\eta_t = \frac{(P_{t,out} - P_{t,in}) \cdot Q}{\tau \cdot \omega} \tag{2}$$

where A_{eff} indicates the effective outlet area. The effective outlet area has to be defined to calculate the effective outlet velocity as shown in Eq. (1). These effective outlet areas are defined in ISO 13350 as shown in Fig. 3 [12]. The (c) definition among three definitions is applied since it has similar shape to jet fan for this study.

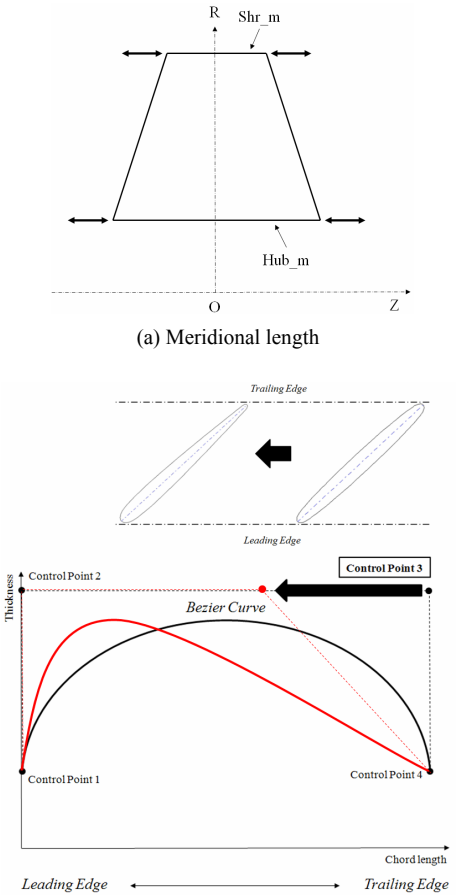

Fig. 4. Definition of the design variables.

The subscripts *in* and *out* refer to the inlet and outlet, respectively; P_t, Q, τ, and ω indicate the total pressure, volumetric flow rate, torque, and angular velocity, respectively.

As mentioned above, although both performance parameters are typically represented with the characteristic of the jet fan having a fixed operating condition, the total efficiency, except the effective outlet velocity, is selected exclusively as the objective function of the numerical optimization.

4.2 Design variables

Table 1 illustrates the main design parameters of the jet fan as previously mentioned. Each angle of the blade at hub and shroud among these parameters depends on the setting angle of the jet fan rotor and affects the effective outlet velocity of the jet fan and the exhaust flow rate. Therefore, we have excluded the blade angles of hub and shroud in this study to satisfy the design flow rate of the jet fan.

In this study, the meridional length (*Hub_m*, *Shr_m*) of hub and shroud influencing the efficiency of the jet fan is selected as the design variable for numerical optimization as shown in Fig. 4(a). Its ranges are set at ±10 mm, considering the restric-

Table 2. Ranges of design variables.

Design	Lower	Base	Upper
Hub_m (mm)	84	94	104
Hub_th (%)	10	55	100
Shr_m (mm)	38.6	48.6	58.6
Shr_th (%)	10	55	100

tive design conditions based on the base model.

As shown in Fig. 4(b), the thickness profile of the jet fan can be expressed to the Bezier curve having the four controls points. When Control Point 3, except for other fixed control points, is moved in the (-) direction horizontally, the maximum thickness moves forward, and the blade shape changes to the airfoil type. Thus, each relative position (*Hub_th*, *Shr_th*) of Control Point 3 at the hub and shroud is selected for the design variables of this study. The ranges of the design variables, *Hub_th* and *Shr_th*, are 10~100%. For example, the relative position of Control Point 3 of the base model, which has a symmetric blade, is 100%. The ranges of the design variables appear in Table 2.

4.3 Latin-hypercube sampling (LHS)

This study newly and randomly generated 35 design points within the design space for 4 design variables with the help of Latin-hypercube sampling (LHS) [13]. The LHS is a matrix m × n order where m is the number of levels (sampling points) to be examined and n is the number of design variables. Each of the n columns of the matrix containing the levels 1, 2, …, m is randomly paired to form the LHS. Therefore, the LHS generates random sample points, ensuring the representation of all portions of the design space.

4.4 PRESS-based-averaging model

This study employs the PRESS (predicted error sum of squares)-based-averaging (PBA) model as a surrogate model to perform design optimization of a tunnel ventilation jet fan. The PBA model, one of the weighted-average surrogate models proposed by Goel et al. [14] and called by Samad et al. [15] is defined based on the PRESS as follows:

$$F_{wt,avg}(x) = \sum_{i}^{N_{SM}} w_i(x) F_i(x) \tag{3}$$

where N_{SM} is the number of basic surrogate models used to construct the PBA model. The surrogate i^{th} at the design point x produces weight $w_i(x)$, and $F_i(x)$ is the predicted response by the i^{th} surrogate model. We can write Eq. (3) in a simplified form as follows:

$$F_{wt,\,avg} = w_{RSA}F_{RSA} + w_{KRG}F_{KRG} + w_{RBNN}F_{RBNN}$$
$$X_j^l < x_j < X_j^u,\ \text{j= 1,2, 3, …,6.} \tag{4}$$

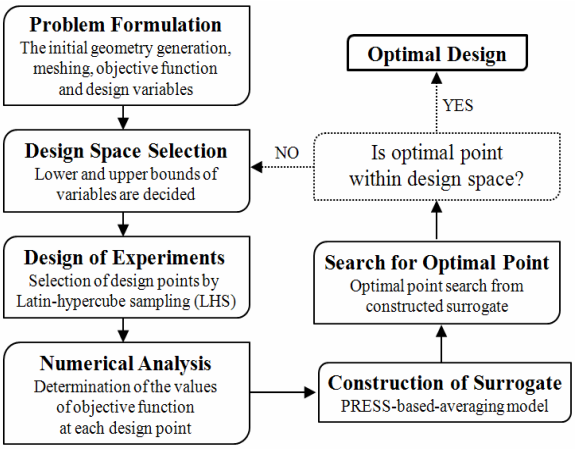

Fig. 5. Optimization procedure.

where, F_{RSA}, F_{KRG} and F_{RBNN} are the responses predicted by the basic surrogates, response surface approximations (RSA), Kriging meta-modeling technique (KRG), and radial basis neural network (RBNN), respectively. Further, X^l and X^u represent the lower and upper bounds on each design variable.

The weights are decided such that the basic surrogate that produces the higher error has the lower weight and, thus, the lower contribution towards the final PBA surrogates and vice-versa. Global weights are calculated from each basic surrogate using generalized mean square cross-validation (CV) error (GMSE) or PRESS (in RSA terminology). In cross-validation, the data is divided into k subsets (k-fold CV) of approximately equal size. The surrogate model is constructed k times, each time leaving out one of the subsets from training and using the omitted subset to compute the error measure of interest. The generalization error estimate is computed using the k error measures obtained (e.g., average). If k equals the sample size, the approach is called leave-one-out CV (or PRESS).

After the PBA surrogate model is constructed, the sequential quadratic programming (SQP) [16] algorithm of optimization is applied to search for the optimum point from the PBA model. Since the SQP depends on the initial guess of the optimum point, a series of trials have been performed before reception of the final optimum point from any surrogate. The flow chart in Fig. 5 describes the overall optimization procedure.

5. Results and discussion

5.1 Validation of the numerical results

Prior to numerical optimization, the result of the numerical analysis is validated by comparison with the experimental data [8] at operating conditions of the jet fan. As shown in Table 3, the numerical results of the effective outlet velocity and the total efficiency of the base model chosen at the same rotational speed are satisfied compared to the experimental data with design specifications of the jet fan. Also, they agree well with the experimental data. We believe that this predicts accu-

Table 3. Comparison of the design specifications, numerical analysis and experiment data.

Design	Specifications	Experiment data	Numerical analysis
N (rpm)	1780		
V_{eff} (m/s)	36.4	36.5	37.9
ηt (%)	68	69.4	70.21

Table 4. Results of the design optimization.

(a) Design variables

Design	*Hub_m* (mm)	*Hub_th* (%)	*Shr_m* (mm)	*Shr_th* (%)
Base	94	100	48.6	100
Optimum	99.39	45.97	48.38	64.4

(b) Objective function values

Design	Prediction (%)	CFD (%)	Increment (%)
Base	-	70.21	-
Optimum	71.42	71.32	1.11

rate results since the computational domain is almost the same as the real model when numerical analysis is performed.

5.2 Results of the numerical optimization

Each weight of the basic surrogates is computed through numerical optimization, and, finally, the simplified form of the PBA model is constituted as follows:

$$F_{wt,\,avg} = 0.584F_{RSA} + 0.396F_{KRG} + 0.020F_{RBNN} \quad (5)$$

where the CV errors are 0.104, 0.203 and 6.117 for the RSA, KRG, and RBNN, respectively. The highest and lowest CV errors are obviously produced by the RBNN and RSA, respectively. As all surrogates do not perform well all the time for all the problems, the PBA surrogate protects designers from using any poor surrogate. The highest weight is assigned to a surrogate that produces the lowest error to construct the PBA surrogate. In the numerical optimization, the highest and lowest weights were assigned to the RSA and RBNN surrogates as these produce the lowest and highest errors, respectively.

Table 4(a) lists the optimum design variables for the present jet fan found by the PBA surrogate model. The total efficiency at operating conditions for the base model is calculated at 70.21%, as shown in Table 4(b). The *Hub_m* is optimized to be a longer shape, while the *Shr_m* is almost same compared to the base model. Also, the *Hub_th* and *Shr_th* are moved forward in comparison to the base model. The total efficiency of the optimum model is estimated at 71.42% by the present optimization and calculated to be 71.32% by RANS analysis. The PBA surrogate model predicts well, with a relative error of 0.1%. Consequently, the present optimization enhances total efficiency by 1.11% compared with the base model.

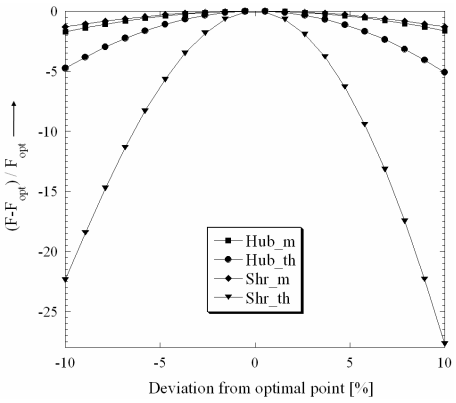

Fig. 6. Sensitivity analysis results.

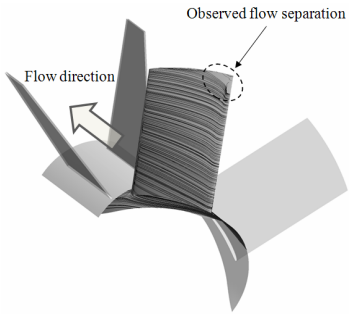

(a) Base model

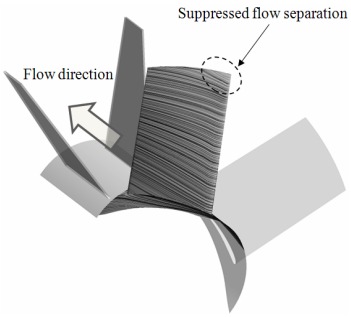

(b) Optimum model

Fig. 7. Limit streamlines comparison at rotor blade.

The sensitivity of the objective function to the design variables is tested as shown in Fig. 6. The variation of each design variable is restricted to ±10% of its optimum value. F_{opt} indicates the objective function value at the optimum point. It shows that the objective function is much more sensitive to the *Shr_th* than to other design variables.

5.3 Comparison of the internal flow fields with the base and optimum models

To evaluate the enhanced efficiency of the jet fan based on the results of numerical optimization, internal flow analyses are performed for the base and optimum models.

Fig. 7 shows the streamline distributions on the blade suction surface of the rotor for the base and optimum models. The

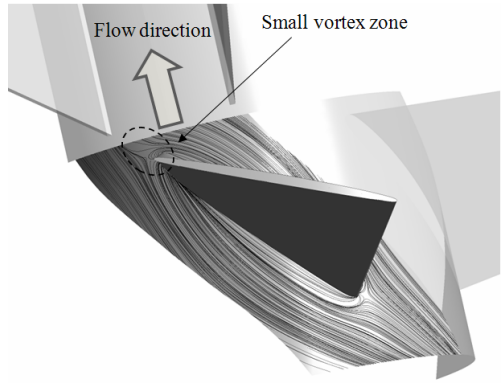

(a) Base model

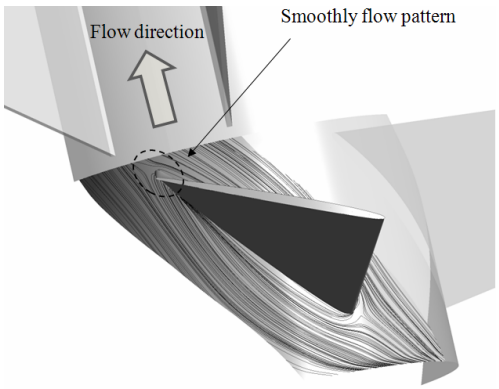

(b) Optimum model

Fig. 8. Limit streamlines comparison at rotor hub.

flow separation is observed on the suction surface of the leading edge near the tip region of the base model. However, the flow separation zone is remarkably suppressed in the optimum model. The authors consider that the flow incidence angle at the inlet changes since the maximum thickness moves forward through the numerical optimization.

Fig. 8 plots the streamline distributions on the hub of the jet fan rotor for the base and optimum models. In the streamline distributions near the downstream region of the jet fan rotor, the optimum model has a smooth flow pattern, while the base model has a small vortex zone. These reveal the reason for the improvement in total efficiency from the influence of the optimized variables.

Fig. 9 shows the tangential velocity vectors near the hub of the trailing edge of the jet fan rotor for the base and optimum models. An observation plane is created to examine the tangential velocity vector near hub of the trailing edge. As shown in Fig. 9, the vortex zone, which causes the efficiency decrease, is observed in the near hub of the trailing edge of the base model. On the other hand, the vortex zone is reduced in the tangential velocity vectors of the optimum model.

6. Conclusion

We conducted optimization techniques based on a PBA surrogate model combined with three-dimensional RANS analysis to improve the total efficiency of a tunnel ventilation jet fan. We can summarize the important conclusions of this study as follows:

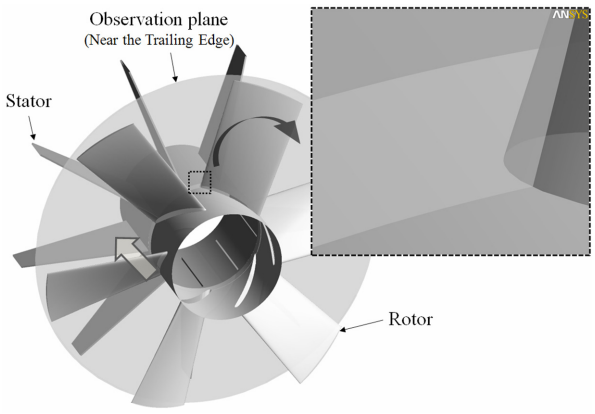

(a) Observation plane

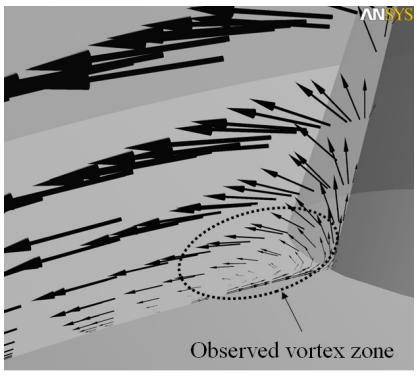

(b) Base model

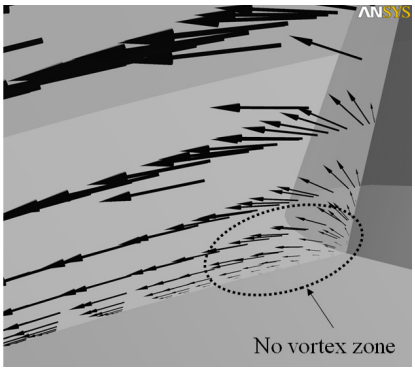

(c) Optimum model

Fig. 9. Tangential velocity vectors near the trailing edge.

(1) The numerical results of the base model are validated in comparison with experimental data at operating conditions. As the results show, they agree well with the experimental data.

(2) The total efficiency of the optimum model is enhanced by 1.11% using the present optimization method as compared with the base model. Given its increased efficiency, we

believe the present optimization method will contribute to reducing operating costs.

(3) To evaluate the enhanced causes of the jet fan efficiency, internal flow analyses are performed for both base and optimum models. The results show remarkable suppression of the flow separation zone in the flow region of the optimum model.

(4) Reversible performance is considered an important performance parameter in a tunnel ventilation jet fan. Therefore, further research should investigate the reversible performance of the tunnel ventilation jet fan.

Acknowledgment

This research was supported by a Korea Institute of Industrial Technology Evaluation and Planning (ITEP) grant funded by the Ministry of Knowledge Economy (No. 10031962).

Nomenclature

A_{eff}	: Efficient outlet area
Hub_m	: Meridional length of hub
Hub_th	: Relative position of the control point 3 at hub
N	: Rotational speed
P_t	: Total pressure
Q	: Volumetric flow rate
Shr_m	: Meridional length of shroud
Shr_th	: Relative position of the control point 3 at shroud
V_{eff}	: Effective outlet velocity
η_t	: Total efficiency
τ	: Torque
ω	: Angular velocity

References

[1] J. H. Ryu, W. H. Yoo and J. Kim, The Jet-fan Model Test for a Road Tunnel Ventilation, *Journal of Air-Conditioning and Refrigeration*, 15 (8) (2003) 630-640.

[2] R. N. Schlaug and T. J. Carlin, Aerodynamics and air quality management of highway tunnels, Prepared Report for Federal Highway Administration USA (1979) 2.49-2.56.

[3] S. Levy, J. Sandzimier, N. Harvey, E. Rosenbluth, K. Karki and S. Patankar, CFD model for transverse ventilation systems, International Conference on Tunnel Fires and One Day Seminar on Escape from Tunnels, Lyons, France (1999) 223-233.

[4] M. Tabarra, E. C. Bennet, R. D. Matthews, J. Armstrong and T. W. Smith, Eccentricity effects on jet fan performance in longitudinally ventilated rectangular tunnels, Paper presented at the I. Mech. E. Seminar Fans for Hazardous Applications, London (1994).

[5] T. Nishioka, M. Jyohkoh and T. Kanno, *Development of high-speed low-noise jet fan for modern tunnel ventilation system*, The 9th Asian International Conference on Fluid Machinery, 9 (56) (2007).

[6] J. S. Byun, S. H. Kang, J. Kim and J. H. Lee, Ventilation analysis according to jet fan location in curved long road tunnel, *Journal of SAREK*, 19 (9) (2007) 615-680.

[7] J. O. Yoo, C. H. Nam and H. J. Shine, The study of jet fan control logic for longitudinal ventilation in road tunnel, *Journal of SAREK*, 12 (8) (2000) 703-790.

[8] S. H. Yang, *Development of high speed compact jet fan*, 2nd Annual report for MKE Strategic Technology Development Project (2010).

[9] J. H. Kim, J. H. Choi, A. Husain and K. Y. Kim, Performance enhancement of axial fan blade through multi-objective optimization techniques, *Journal of Mechanical Science and Technology*, 24 (10) (2010) 2059-2066.

[10] Y. S. Choi, J. H. Kim, K. Y. Lee and S. H. Yang, Performance improvement of high speed jet fan, *International Journal of Fluid Machinery and System*, 3 (1) (2010) 39-49.

[11] S. H. Yang, *Development of high speed compact jet fan*, 1st Annual report for MKE Strategic Technology Development Project (2009).

[12] ISO 13350, Industrial fans-performance testing of jet fans, INTERNATIONAL STANDARD (1999) 2-5.

[13] JMP 6.0.0, The statistical discovery software, version 6.0.0, SAS Institute Inc., Cary, NC, USA (2005).

[14] T. Goel, R. T. Haftka, W. Shyy and N. V. Queipo, Ensemble of surrogates, *Structural and Multidisciplinary Optimization*, 33 (3) (2007) 199-216.

[15] A. Samad, K. Y. Kim, Goel, T. R. T. Haftka and W. Shyy, Multiple surrogate modeling for axial compressor blade shape optimization, *Journal of Propulsion and Power*, 24 (2) 302-310.

[16] MATLAB®, The language of technical computing, Release 14, The Math Works Inc. (2004).

Joon-Hyung Kim received his B.S. and M.S. degrees from Hanyang University, Korea, in 2005 and 2007, respectively. He is pursuing his research towards the Ph.D in Fluid Mechanics at Hanyang University. And he is currently a researcher in the Korea Institute of Industrial Technology (KITECH). His research interests are computational fluid dynamics and design optimization of turbomachinery.

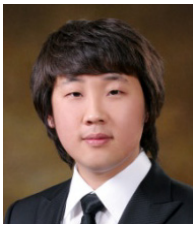

Jin-Hyuk Kim received his B.S. from Sunmoon University, Korea, in 2007, and his M.S, degree from Inha University, Korea, in 2009. Currently he is pursuing his research towards Ph.D degree in Thermodynamics and Fluid Mechanics at the Inha University. His research interests include design of turbomachinery, numerical analyses and optimization techniques.

Kwang-Yong Kim received the B.S. degree from Seoul National University in 1978, and the M.S. and Ph.D from the Korea Advanced Institute of Science and Technology (KAIST), Korea in 1981 and 1987, respectively. He is currently an Inha Fellow Professor in the School of Mechanical Engineering of the Inha University, Incheon, Korea. Professor Kim is also the current Editor-in-Chief of the *International Journal of Fluid Machinery and Systems* (IJFMS). He is a Fellow of the American Society of Mechanical Engineers (ASME) and an Associate Fellow of the American Institute of Aeronautics and Astronautics (AIAA).

Joon-Yong Yoon received his B.S. and M.S. degrees from the Hanyang University and Ph.D from the Univ. of Iowa in Mechanical Engineering. He is a professor of Mechanical Engineering at Hanyang University. His research areas are in CFD for applications, renewable energy, MEMS and flow control.

Sang-Ho Yang received his B.S. and M.S. degrees from the Korea Polytechnic University, in 2006 and 2008, He is concurrently a Ph.D candidate at Korea Polytechnic University. And he is a director in the Samwon E&B. His research interests are in design and experiment of fans.

Young-Seok Choi received his B.S. degree from Seoul National University in 1988, and his M.S. and Ph.D in Mechanical Engineering at the same university in 1990 and 1996, respectively. He is currently a principal researcher in KITECH. His research interests are in computational fluid dynamics and design optimization of turbomachinery.